JOURNAL OF MAGNETIC RESONANCE **133,** 200–203 (1998)
ARTICLE NO. MN981441

COMMUNICATIONS

Fast Broadband Inversion by Adiabatic Pulses

Tsang-Lin Hwang,*,[1] Peter C. M. van Zijl,* and Michael Garwood†

*Johns Hopkins University School of Medicine, Department of Radiology and Biophysics and Biophysical Chemistry, 217 Traylor Building, 720 Rutland Avenue, Baltimore, Maryland 21205, and †Center for Magnetic Resonance Research and Department of Radiology, University of Minnesota Medical School, Minneapolis, Minnesota 55455

Received November 6, 1997

Despite the advantages of compensation for resonance offset and B_1 inhomogeneity, adiabatic pulses are not yet in general use in high-resolution NMR, often because of the conception that these pulses require longer time or increased power to perform. We show that adiabatic pulses with tangential frequency sweeps and other frequency-modulation functions can be optimized to accomplish ^{13}C and ^{1}H broadband inversion using pulse lengths of 192 and 64 μs, respectively, at B_1 strengths available with modern high-resolution probes. © 1998 Academic Press

Key Words: **adiabatic pulses; fast broadband inversion; tangential frequency sweep.**

Broadband inversion pulses are key elements in many NMR experiments. An enormous amount of effort has been put into the design of composite pulses (*1–4*) and adiabatic full passages (AFPs) (*5–7*) to simultaneously compensate resonance offset and B_1 inhomogeneity for better inversion. Although AFPs can invert across wider bandwidths and have higher tolerance to B_1 inhomogeneity as compared to the best composite pulses operating with the same RF power, AFPs are usually considered to require much more time to perform. Nonetheless, AFPs have recently gained popularity in high-resolution NMR for low-powered ^{13}C broadband decoupling (*8–11*), ^{13}C inversion (*12, 13*), and refocusing without phase distortion (*14, 15*). For many high-resolution applications, especially the study of macromolecules, it is important to achieve short pulse durations to avoid T_2 losses. A recent report by Stott *et al.* (*16*) describes a frequency-modulated broadband inversion pulse which employs a WURST-20 amplitude function (*9*) and a nonlinear frequency sweep. With $\gamma B_1^{\max} =$ 15.6 kHz and a pulse duration of only 192 μs, this pulse achieves 99.5% inversion over a bandwidth approximately equal to 15 kHz, and tolerates RF amplitude variations up to $\pm 30\%$ $B_1^{\max}$. This pulse was designed to achieve near-perfect inversion across the proton chemical shift range, as required in DPFGSE NOE experiments (*17*) to detect small NOEs. Instead of using a linear frequency sweep, others have shown the efficiency of using the tangential frequency sweep for spin inversion (*5, 7*). In this Communication, we extend and optimize the use of tangential frequency sweeps and other modulation functions to accomplish ^{13}C and ^{1}H broadband inversion using pulse lengths $T_p = 192$ and 64 μs, respectively, and B_1 strengths readily available with modern high-resolution probes.

An AFP can employ different combinations of amplitude modulation (AM) and frequency modulation (FM), which can be written as

$$\boldsymbol{\omega_1}(t) = \gamma B_1^{\max} F_1(t)\hat{\mathbf{x}}' \qquad [1]$$

$$\boldsymbol{\Delta\omega}(t) = [\omega_0 - \omega(t)]\hat{\mathbf{z}}' = [\Omega - AF_2(t)]\hat{\mathbf{z}}' \qquad [2]$$

where $B_1^{\max}$ and A are the amplitudes of $B_1(t)$ and of the frequency sweep (relative to the central carrier frequency ω_c), $F_1(t)$ and $F_2(t)$ are dimensionless functions describing the amplitude and frequency modulation with values in the range of 0 to 1 and -1 to 1, respectively, γ is the gyromagnetic ratio, and $\Omega = \omega_0 - \omega_c$, where ω_0 is the Larmor frequency of an isochromat. Equations [1] and [2] describe the frequency components in the so-called FM frame (*5*), which rotates at the instantaneous frequency of the pulse, $\omega(t)$. In the FM frame, $\boldsymbol{\omega_1}(t)$ is fixed in the $\hat{\mathbf{x}}'$ direction. The effective magnetic field $\mathbf{B}_\Omega^{\text{eff}}(t)$, experienced by an isochromat at offset Ω and time t, is the vector sum of the field components, $\mathbf{B}_1(t)$ and $\boldsymbol{\Delta\omega}(t)/\gamma$. For the time interval equal to the pulse duration T_p, and for the offset interval $|\Omega| < A$, the adiabatic condition can be defined as (*18*)

$$K(\Omega, t) = \left| \frac{\gamma B_\Omega^{\text{eff}}(t)}{\dot{\alpha}} \right| = \frac{A^2[(\gamma B_1^{\max} F_1(t)/A)^2 + (F_2(t) - \Omega/A)^2]^{3/2}}{\gamma B_1^{\max} |(F_2(t) - \Omega/A)\dot{F}_1(t) - F_1(t)\dot{F}_2(t)|} \gg 1, \qquad [3]$$

where $\dot{\alpha}$ is the rate of change of the $\mathbf{B}_\Omega^{\text{eff}}(t)$ orientation. If the adiabatic condition is satisfied, an isochromat follows the trajectory of $\mathbf{B}_\Omega^{\text{eff}}(t)$ during an AFP, resulting in inversion. The

[1] To whom correspondence should be addressed.

1090-7807/98 $25.00

most critical adiabatic condition occurs when an isochromat is on resonance, that is, $F_2(t_\Omega)=\Omega/A$, at the specific time $t = t_\Omega$,

$$K(t_\Omega) = \frac{[\gamma B_1^{\max} F_1(t_\Omega)]^2}{A\dot{F}_2(t_\Omega)}, \qquad [4]$$

where $B_\Omega^{\text{eff}}(t_\Omega)$ has the minimum value equal to the transverse field $B_1^{\max}F_1(t_\Omega)$. If $K(t_\Omega)$ is constant for isochromats at different offsets Ω, Eq. [4] provides the recipe to construct AFP pulses with offset-independent adiabaticity (*18, 19*). When the AM function is specified, the FM function can be obtained by taking the time integral of the square of this AM function.

The well-known hyperbolic secant (HS) pulse (*5, 6*) is one example of a pulse possessing offset-independent adiabaticity. In some circumstances, however, peak power limitations may be encountered when a sech function is used to modulate B_1. To reduce peak power, Tannús and Garwood (*18*) proposed raising the time variable in the sech function to a higher *n*th power. According to Eq. [4], the longitudinal modulation in the FM frame becomes

$$\Delta\boldsymbol{\omega}(t) = [\Omega - A\int_0^\tau \text{sech}^2(\beta\tau'^n)d\tau']\hat{\mathbf{z}}', \qquad [5]$$

where $\tau\,(=2t/T_p)$ is defined in the interval $-1 \le \tau \le 1$, and the truncation factor β is chosen such that $\text{sech}(\beta) = 0.01$. These pulses have been dubbed HS*n*. For current spectrometers equipped with pulse shaping capabilities, the frequency modulation is usually implemented in terms of the phase modulation, obtained by integrating the FM function with respect to time. Figure 1a shows the modulation functions of HS4, with phase-modulated function $\phi(t)$.

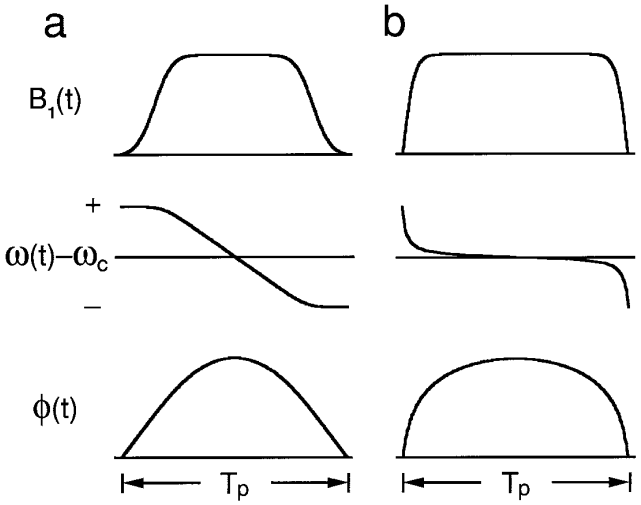

FIG. 1. Inversion pulses for (a) HS4 and (b) tanh/tan. $B_1(t)$, $\omega(t) - \omega_c$, and $\phi(t)$ represent the shapes of their amplitude-modulated, frequency-modulated, and phase-modulated functions, respectively. T_p is the pulse length.

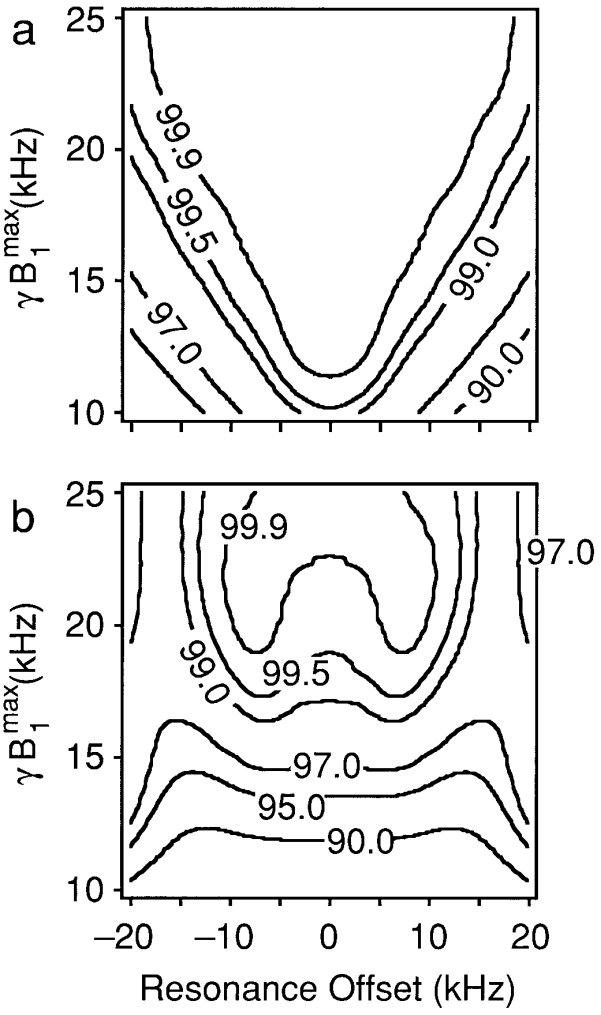

FIG. 2. Simulated inversion contours of (a) [tanh/tan, $R = 110$] and (b) [HS4, $R = 14$] as a function of resonance offsets and $\gamma B_1^{\max}$. T_p for both pulses is 192 μs.

Another kind of AFP employs the pair of hyperbolic tangent (tanh) and tangent (tan) functions (Fig. 1b), which do not satisfy the criteria for the offset-independent adiabaticity. This AFP can be constructed from an adiabatic half passage (AHP) and its time-reversed adiabatic half passage. The first AHP can be written as (*20, 21*)

$$\boldsymbol{\omega}_1(t) = \gamma B_1^{\max}\tanh[\xi 2t/T_p]\hat{\mathbf{x}}' \qquad [6]$$

$$\Delta\boldsymbol{\omega}(t) = \left[\Omega - A\frac{\tan[\kappa(1 - 2t/T_p)]}{\tan[\kappa]}\right]\hat{\mathbf{z}}', \qquad [7]$$

where $\xi = 10$, $\tan[\kappa] = 20$, and $0 \le t \le T_p/2$ are used. The tanh/tan combination has been applied to construct adiabatic B_1-insensitive rotation (BIR) pulses that can perform rotations for any flip angle (*20*). The phase-modulated form of Eq. [7] is

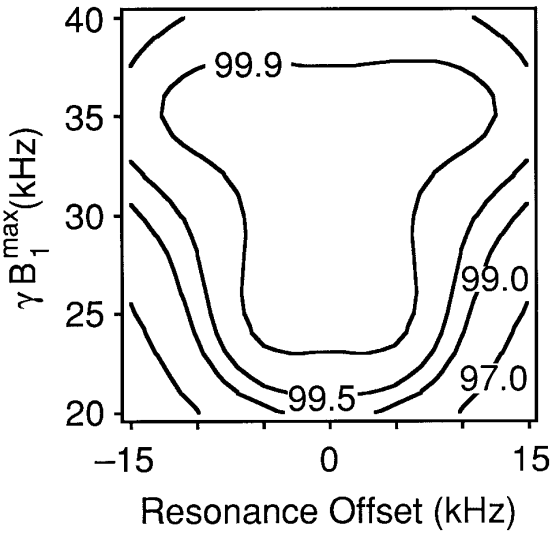

FIG. 3. Simulated inversion contours of [tanh/tan, $R = 54$] as a function of resonance offsets and γB_1^{max}. $T_p = 64$ μs.

$$\phi(t) = \phi_{max} - \frac{AT_p}{2\kappa \tan[\kappa]} \ln\left(\frac{\cos[\kappa(1 - 2t/T_p)]}{\cos \kappa}\right), \quad [7]$$

where

$$\phi_{max} = -\frac{AT_p}{2\kappa \tan[\kappa]} \ln(\cos \kappa). \quad [8]$$

To describe AFP pulses, a convenient unitless parameter R can be defined as (*11, 22*)

$$R = A \cdot T_p/\pi = \text{bw} \cdot T_p, \quad [9]$$

where bw is the pulse bandwidth in hertz and T_p is the pulse length in seconds. The nomenclature used here to describe each AFP is [AM/FM functions, R value used to construct the pulse].

For tanh/tan and HS4, B_1 amplitudes at both extremes are zero or close to zero, respectively. At the beginning and end of these pulses, the magnitude of γB_Ω^{eff} is dominated by $\Omega + A$ and $\Omega - A$, respectively, and the orientation of $\mathbf{B}_\Omega^{eff}$ is approximately collinear with the longitudinal axis for isochromats $|\Omega| < A$. Thus, the effective field starts out collinear with the longitudinal magnetization, and the degree of inversion for an isochromat Ω is limited only by the ability to achieve the adiabatic condition. For HS4, the frequency sweep rate is low at the extremes of the pulse where $B_1(t)$ is small (Fig. 1a). This latter property of HS4 is required to achieve offset-independent adiabaticity. In contrast, it can be seen that the rate of the tangential frequency sweep is high at the extremes where $B_1(t)$ is still small (Fig. 1b). Thus, the adiabatic condition is more difficult to satisfy for isochromats precessing near the extremes of the tangential frequency sweep, but the adiabatic condition can be well satisfied for isochromats in the central portion of the sweep. For this reason, a much higher R-value is needed for the tanh/tan pulse when comparing its working bandwidth with that of HSn pulses of the same duration.

With the help of simulations, we first set the AFP pulse lengths of tanh/tan and HSn to 192 μs, and then optimize the R values while observing their performance. The inversion efficiency is calculated according to $1/2(1-M_z/m_z) \times 100\%$ (*14*), where m_z is the unit vector, positioned along the longitudinal axis at the start of calculation, and M_z is the z component of the vector after applying the pulse. Relaxation is ignored during the calculation. Figure 2a shows the inversion performance of [tanh/tan, $R = 110$]. As B_1^{max} increases, a wider range of isochromats satisfy the adiabatic condition and become completely inverted. For HSn pulses, n and R can both be varied to have different performance. Figure 2b presents the inversion efficiency when $n = 4$ and $R = 14$. At low γB_1^{max} settings (e.g., < 16 kHz), [HS4, $R = 14$] achieves broader inversion bandwidth than [tanh/tan, R 110]. However, when more peak power is available, [tanh/tan, $R = 110$] produces a wider complete inversion. To further demonstrate the principle, we reduced the pulse length for tanh/tan AFP. Figure 3 shows the inversion efficiency for [tanh/tan, $R = 54$] using $T_p = 64$ μs. At γB_1^{max} between 25 and 35 kHz, this pulse covers >18 kHz bandwidth with $\geq 99.5\%$ inversion, sufficient for the proton chemical shift range. Table 1 lists the inversion efficiency and associated bandwidths at different γB_1^{max} values for [HS4, $R = 14$], [tanh/tan, $R = 110$], and [tanh/tan, $R = 54$].

These sequences were all implemented on a Varian UnityPlus 500-MHz spectrometer equipped with a 5-mm triple-resonance PFG probe, RF waveform generators and a shielded z-gradient unit. Inversion experiments, {180°–G–90°–acquire}, were performed on a sample of 1% H_2O in D_2O, doped with 0.1 mg/ml $GdCl_3$. Figure 4 compares the inversion performance of [tanh/tan, $R = 110$] and [HS4, $R = 14$], both with 192 μs duration, and of the 90(x) 240(y) 90(x) composite pulse (*23*), all with $\gamma B_1^{max} = 20.0$ kHz. The results agree with the simulations in showing that [tanh/tan, $R = 110$] can almost completely invert isochromats across 40 kHz bandwidth, which should be adequate for the ^{13}C bandwidths at most field strengths. The experimental inversion

TABLE 1
Calculated Bandwidth in Kilohertz for Three Different Inversion Efficiencies at Various γB_1^{max} Values

Pulse	T_p (μs)	γB_1^{max} (kHz)	99.5%[a]	99%[a]	95%[a]
HS4, $R = 14$	192	16	[b]	[b]	53
		20	20	28	47
tanh/tan, $R = 110$	192	16	25	30	42
		20	36.5	41	54
tanh/tan, $R = 54$	64	25	18	21.5	34.5
		35	32.5	37	51

[a] Inversion efficiency.
[b] The inversion efficiency is below 99%.

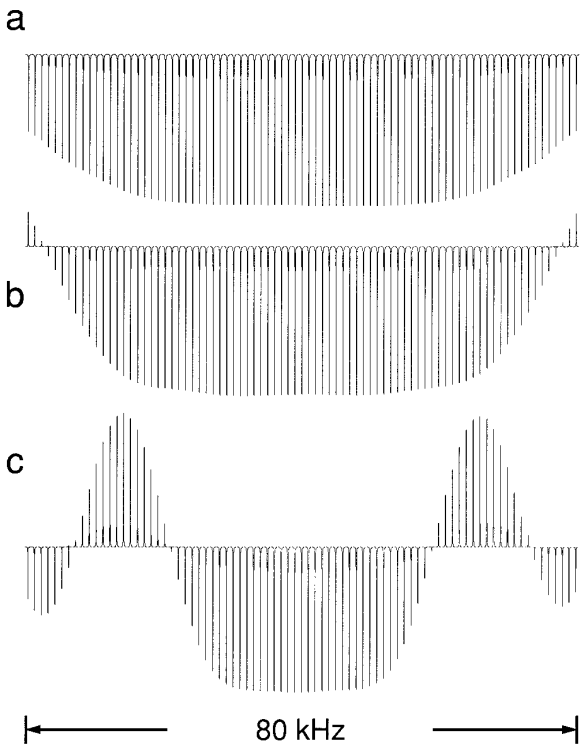

FIG. 4. Experimental inversion profiles of (a) [tanh/tan, $R = 110$], (b) [HS4, $R = 14$], and (c) 90(x) 240(y) 90(x), all obtained at $\gamma B_1^{\max} = 20.0$ kHz. $T_p = 192$ μs for (a) and (b), and 58.3 μs for (c). The resonance offsets were stepped from −40 to 40 kHz in increments of 1 kHz.

data obtained from the [tanh/tan, $R = 54$] pulse with 64 μs duration at various $\gamma B_1^{\max}$ (not shown) is also in agreement with the simulated result (Fig. 3).

In conclusion, we have shown that fast broadband inversion can be achieved for several AFP pulses, including the tanh/tan pulse. Other applications of AFP pulses should also benefit from similar optimizations of pulse parameters in consideration of the peak power, pulse length limitations, inversion efficiency, and bandwidth requirements of the experiment.

ACKNOWLEDGMENTS

This research was supported by NIH Grants RR11115 (PvZ) and RR08079 (MG), and, in part, via a subcontract of NIH STTR Grant GM55441 to Adiabatics, Inc., of which M.G. and P.v.Z. are officers. The terms of this agreement have been reviewed and approved by the Johns Hopkins University in accordance with its conflict of interest policies.

REFERENCES

1. M. H. Levitt, Composite pulses, *Prog. NMR Spectrosc.* **18,** 61–122 (1986).
2. A. J. Shaka and J. Keeler, Broadband spin decoupling in isotropic liquids, *Prog. NMR Spectrosc.* **19,** 47–129 (1987).
3. T. Fujiwara, T. Anai, N. Kurihara, and K. Nagayama, Frequency-switched composite pulses for decoupling carbon-13 spins over ultrabroad bandwidths, *J. Magn. Reson. A* **104,** 103–105 (1993).
4. D. Abramovich and S. Vega, Derivation of broadband and narrowband excitation pulses using the Floquet formalism, *J. Magn. Reson. A* **105,** 30–48 (1993).
5. J. Baum, R. Tycko, and A. Pines, Broadband and adiabatic inversion of a two-level system by phase-modulated pulses, *Phys. Rev. A* **32,** 3435–3447 (1985).
6. M. S. Silver, R. I. Joseph, and D. I. Hoult, Highly selective $\pi/2$ and π pulse generation, *J. Magn. Reson.* **59,** 347–351 (1984).
7. C. J. Hardy, W. A. Edelstein, and D. Vatis, Efficient adiabatic fast passage for NMR population inversion in the presence of radiofrequency field inhomogeneity and frequency offsets, *J. Magn. Reson.* **66,** 470–482 (1986).
8. M. R. Bendall, Broadband and narrowband spin decoupling using adiabatic spin flips, *J. Magn. Reson. A* **112,** 126–129 (1995).
9. Ē. Kupče and R. Freeman, Adiabatic pulses for wideband inversion and broadband decoupling, *J. Magn. Reson. A* **115,** 273–276 (1995).
10. R. Fu and G. Bodenhausen, Ultra-broadband decoupling, *J. Magn. Reson. A* **117,** 324–325 (1995).
11. T.-L. Hwang, M. Garwood, A. Tannús, and P. C. M. van Zijl, Reduction of sideband intensities in adiabatic decoupling using modulation generated through adiabatic *R*-variation (MGAR), *J. Magn. Reson. A* **121,** 221–226 (1996).
12. K. Hallenga and G. M. Lippens, A constant-time ^{13}C–^{1}H HSQC with uniform excitation over the complete ^{13}C chemical shift range, *J. Biomol. NMR* **5,** 59–66 (1995).
13. K. Ogura, H. Terasawa, and F. Inagaki, Fully ^{13}C-refocused multidimensional ^{13}C-edited pulse schemes using broadband shaped inversion and refocusing pulses, *J. Magn. Reson. B* **112,** 63–68 (1996).
14. T.-L. Hwang and A. J. Shaka, Water suppression that works. Excitation sculpting using arbitrary waveforms and pulsed field gradients, *J. Magn. Reson. A* **112,** 275–279 (1995).
15. T.-L. Hwang, P. C. M. van Zijl, and M. Garwood, Broadband adiabatic refocusing without phase distortion, *J. Magn. Reson.* **124,** 250–254 (1997).
16. K. Stott, J. Keeler, Q. N. Van, and A. J. Shaka, One-dimensional NOE experiments using pulsed field gradients, *J. Magn. Reson.* **125,** 302–324 (1997).
17. K. Stott, J. Stonehouse, J. Keeler, T.-L. Hwang, and A. J. Shaka, Excitation sculpting in high-resolution nuclear magnetic resonance spectroscopy: Application to selective NOE experiments, *J. Am. Chem. Soc.* **117,** 4199–4200 (1995).
18. A. Tannús and M. Garwood, Improved performance of frequency-swept pulses using offset-independent adiabaticity, *J. Magn. Reson. A* **120,** 133–137 (1996).
19. Ē. Kupče and R. Freeman, Optimized adiabatic pulses for wideband spin inversion, *J. Magn. Reson. A* **118,** 299–303 (1996).
20. M. Garwood and Y. Ke, Symmetric pulses to induce arbitrary flip angles with compensation for RF inhomogeneity and resonance offsets, *J. Magn. Reson.* **94,** 511–525 (1991).
21. M. Garwood and K. Ugurbil, B_1 insensitive adiabatic RF pulses, *in* "NMR, Basic Principles and Progress," (M. Rudin, Ed.) Vol. 26, pp. 109–147, Springer-Verlag, Berlin (1992).
22. Y. Ke, D. G. Schupp, and M. Garwood, Adiabatic DANTE sequences for B_1-insensitive narrowband inversion, *J. Magn. Reson.* **96,** 663–669 (1992).
23. R. Freeman, S. P. Kempsell, and M. H. Levitt, Radiofrequency pulse sequences which compensate their own imperfections, *J. Magn. Reson.* **38,** 453–479 (1980).